Nanocrystalline ZrO_2 thin films on silicon fabricated by pulsed-pressure metalorganic chemical vapor deposition (PP-MOCVD)

L. Ramirez[a] and M.L. Mecartney
Department of Chemical Engineering and Materials Science, University of California–Irvine, Irvine, California 92697-2575

S.P. Krumdieck
Department of Mechanical Engineering, University of Canterbury, Christchurch, Private Bag 4800, Christchurch, New Zealand

(Received 11 January 2008; accepted 5 May 2008)

ZrO_2 films deposited on silicon (100) substrates using pulsed-pressure metalorganic chemical vapor deposition (PP-MOCVD) with zirconium n-propoxide (ZnP) $Zr(OC_3H_7)_4$ were dense and fully crystalline for substrate temperatures of 500 to 700 °C. Film thicknesses were 40 to 815 nm thick, measured after growth using ellipsometry and scanning electron microscopy (SEM). The growth rate was between 0.1 μm/h at 500 °C and 1 μm/h at 700 °C. Transmission electron microscopy (TEM) and x-ray diffraction (XRD) indicated an average grain size of 10 to 20 nm. There was a random orientation of cubic/tetragonal zirconia at the highest experimental temperature of 700 °C. SEM and atomic force microscopy (AFM) was used to characterize island height of discontinuous films in the initial stages of growth where defects in the substrate caused preferred nucleation of isolated particles. At later stages of growth, the average surface roughness of continuous films was 30 nm, which revealed a more uniform growth had developed. A growth model is proposed, and optimal growth conditions are suggested for targeted microstructures of ZrO_2 films.

I. INTRODUCTION

The ability to tailor material microstructures by controlling zirconia film growth is highly desirable for a broad range of technological applications, from building microelectronics to creating solid-oxide electrolytes. Currently, a variety of deposition techniques are used to achieve the diverse material characteristics and microstructures required for different applications. Ultrathin films of zirconia on Si for high-k dielectric films can be made by rapid thermal chemical vapor deposition (CVD),[1] atomic layer deposition (ALD),[2] ultraviolet (UV)-ozone oxidation of Zr metal,[3] or specialized sputtering techniques.[4,5] Line-of-sight techniques such as electron beam physical vapor deposition (EB-PVD)[6,7] and air plasma spraying (APS)[8–10] are fabrication methods typically used in the deposition of zirconia for thermal-barrier coatings (TBC)[11]; however, the complex geometries of high-temperature components such as gas turbine blades make line-of-sight methods challenging to use for uniform deposition. Screen printing is currently used for thick-film solid-oxide fuel cell (SOFC) planar electrolytes.[12] However, as SOFC electrolytes are scaled down to thin films for enhanced efficiency, the fabrication of dense gas-impermeable materials becomes critical and alternative deposition techniques may be required. One option is CVD, a type of processing that can produce thin films on conformal surfaces. Low-pressure CVD, low-temperature kinetic-controlled CVD, and ALD all produce films with good uniformity, but also are methods with inherently slow deposition rates.

Pulsed-pressure metalorganic chemical vapor deposition (PP-MOCVD) is a specialized CVD technique that modulates incubation time so deposition processes happen in sequence rather than simultaneously.[13] Regulating this period of "relaxation time," i.e., the time a precursor molecule resides in the reaction chamber, allows for the tailoring of the process to produce a target microstructure. Among the many advantages of using PP-MOCVD compared with conventional CVD are a lower-cost manufacturing route for oxide coatings and functional layers, a very high conversion efficiency (up to 90%) that results in much lower concentrations of waste by-products, and highly competitive growth rates (up to

[a]Address all correspondence to this author.
e-mail: lynher@uci.edu
DOI: 10.1557/JMR.2008.0267

10 μm/h) for yttria-stabilized zirconia (YSZ) compared with other vapor-phase deposition techniques.[14]

Rapid growth rates with PP-MOCVD are possible primarily due to the pulsing of the liquid organometallic precursor that is delivered directly into the reaction chamber using an ultrasonic nozzle to create a fine spray (droplet diameter <20 μm). In this system, growth rates are not limited by the precursor evaporation rate or diffusion through a carrier gas. During the PP-MOCVD process, droplets flash evaporate into vapor that disperses rapidly in the evacuated reactor, producing a uniform concentration of precursor and solvent vapor, approximating well-stirred reactor conditions. The vaporized precursor molecules react at the surface of a heated substrate and decompose to form metal oxides. (Note that zirconium–oxygen bonds already exist in the alkoxide precursor molecules.) The chamber is pumped down, and the next pulse of liquid delivery begins within 10 s.

Nucleation is influenced by the peak pulse pressure, which determines the maximum molecular arrival rate. The reactor pressure drops rapidly (rate depends on vacuum pumping speed), but the gas diffusivity increases with decreasing pressure, resulting in effectively an active "selective pumping" of the precursor as it is adsorbed and consumed on the substrate.[14,15] The integral of the arrival rate over the pulse peak is called the exposure. As with all other MOCVD processes, the maximum growth rate is a strong function of temperature and the precursor properties. The growth rate maximum is expected where the temperature is high enough that the precursor reaction rate is faster than the adsorption rate, but not so high as to decrease adsorption.

Products and solvent vapor are actively removed during the exhaust pump-down part of the cycle. As the pressure drops, additional adatoms diffuse across to the growing crystal surfaces and become incorporated into the crystal lattice. After the reactor has been pumped down to the base pressure, a relaxation time can be set before the next pulse. During this time, no new adatoms come to the surface while the crystal is assembling. The thermal decomposition of the precursor molecule is the rate-limiting step for CVD zirconia film growth and is crucial to the subsequent chemical reaction and crystal growth of zirconia onto the substrate.[16] The maximum arrival rate, total pulse exposure, relaxation time, surface diffusion, and adatom incorporation energetics are all factors that will determine the microstructure of the film deposited and are all factors that, to a large degree, can be controlled with PP-MOCVD.

Despite the usefulness of both conventional CVD and PP-MOCVD as thin-film deposition techniques, there has been relatively little research on the early stages of nucleation and growth in the CVD process. Understanding how process parameters affect the early stages of nucleation and growth should lead to better control of the film microstructure. Kajikawa and Noda[17] introduced the key concept that incubation time in CVD reactors can influence microstructural development. Cameron and George[16] determined that zirconium alkoxide decomposition is the rate-limiting step for CVD zirconia film growth using alkoxide precursors. However, the study of the nucleation and growth processes is inherently difficult with conventional steady-flow MOCVD as the process cannot easily be arrested just after initiation, nor can the first few moments of deposition be readily observed in situ. Additionally, the arrival rates in conventional MOCVD are highly dependent on details of the viscous boundary layer and local concentration gradients and thus are difficult to determine or control. This paper aims to advance existing knowledge of critical CVD processes by evaluating microstructural evolution of zirconia PP-MOCVD thin films on silicon as a function of precursor volume (shot size), the number of pulses, and substrate temperature, taking snapshots of film growth at various stages of the process.

II. EXPERIMENTAL PROCEDURE

Zirconia films were grown on n-type Si (100) substrates using a PP-MOCVD system described in detail elsewhere.[18] In this procedure, a 1 mol% solution of zirconium n-propoxide in n-propanol was used as a single source metalorganic precursor. Zirconium n-propoxide was chosen as the precursor to ZrO_2 because of its pre-existing oxygen bond to zirconium, its relatively high volatility, and its low cost.[19,20]

Maximum temperature was determined by the upper limits of the ceramic heater, which provided substrate temperatures ranging from 500 to 700 °C as measured by a k-type thermocouple. The thermocouple was located inside a metal susceptor plate onto which the silicon sample was placed. The number of pulses was varied from 1 to 300 to observe initial stages of nucleation and growth in the low-pulse regime and to provide complete film coverage for higher-pulse experiments. The PP-MOCVD reactor chamber was pumped down to a base pressure (P_{min}) of 250 Pa and, using precursor shot volumes of either 20 or 50 μL, P_{max} was 320 to 780 Pa, determined by the volume and concentration of precursor shot. A summary of the relevant process parameters for the films produced is given in Table I.

Zirconia film thickness, microstructure, composition, and morphology were characterized using x-ray diffraction (XRD), scanning electron microscopy (SEM), energy-dispersive spectroscopy (EDS), transmission electron microscopy (TEM), and atomic force microscopy (AFM). XRD data were generated using a Siemens/Bruker D-5000 powder diffractometer with a copper source to confirm the formation of zirconia and determine the resultant crystallographic structure. XRD was

TABLE I. List of PP-MOCVD zirconia samples using zirconium propoxide precursor (on silicon substrate).

T (°C)	No. of pulses	P_{min} (Pa)	P_{max} (Pa)	Shot vol (mL)
570	78	265	530	50
600	80	250	500	50
500	300	250	500	50
620	300	240	550	50
655	300	250	600	50
700	300	250	600	50
500	1	250	320	20
700	1	250	510	50
700	1	500	780	50
685	15	250	645	50
700	15	20	330	20

configured for glancing angle (4°) thin-film XRD to maximize signal from film rather than the Si (100) substrate. SEM images were taken on both a Philips XL30 FE-SEM with a secondary electron detector and on a Zeiss Ultra 55 FE-SEM with Gemini column In-Lens and backscatter detector. Analysis of plan-view SEM images was used to determine the grain size using ImageJ software.[21] Grains were outlined, and area calculations led to diameters that were multiplied by a volumetric correction factor of 1.74. EDS data were gathered by Industrial Research Limited (IRL) in New Zealand. TEM images were taken using a Philips CM 20 TEM system. TEM cross sections were prepared using a technique outlined by Weaver.[22] AFM was performed using a Nano-DST from Pacific Nanotechnology, in Irvine, CA.

III. RESULTS AND DISCUSSION

A. Zirconia crystal phase

A set of thin films over a range of deposition temperatures was produced (300 pulse exposures, 50 μL shot volume, and 1 mol% concentration precursor solution). These experiments produced uniform films with thicknesses in the range of several hundred nanometers. XRD resultant plots are shown in Fig. 1. Only the cubic/tetragonal phase of zirconia is observed in the diffraction data, with no monoclinic peaks except a possible trace of the monoclinic phase at 28° for the 620 °C sample [Fig. 1(a)]. It was not possible to conclusively determine whether samples were cubic or tetragonal because of the peak overlap for these phases, but no splitting of peaks at (220) or (400) were observed, which would be expected if $a \neq c$. The absence of any strong monoclinic peaks in the XRD data differs from published results of other MOCVD zirconia films using zirconium *tert*-butoxide precursor,[16,23,24] which report mixtures of cubic/tetragonal and monoclinic phases are the most common products by nonpulsed techniques.

The peak intensities from XRD indicate some preferred orientation at lower temperatures. The powder diffraction file (PDF) for cubic and tetragonal ZrO_2[25] has the highest intensity peak for (111) planes and the second most intense is (220). By comparing relative intensities of (111) at $2\theta \approx 30°$ and (220) at 50° in each sample with these PDF data, it appears that growth of the (111) orientation is suppressed and growth of (110) is enhanced at substrate temperatures of 620 to 650 °C. (110) provides a charge-neutral surface for zirconia. Preferred orientation has also been observed in other CVD ZrO_2 systems. At temperatures of 600 to 800 °C, with low atom mobility, preferred (100) orientation has been observed with low density (100) planes growing the fastest.[26] At higher temperatures (900 °C), (111) planes with the lowest surface energy are dominant in films produced by some CVD systems.[26] At the highest experimental temperature (700 °C) for PP-MOCVD in this work; however, the XRD data in Fig. 1 do not indicate any preferred orientation, but rather a random orientation in agreement with the PDF.[25]

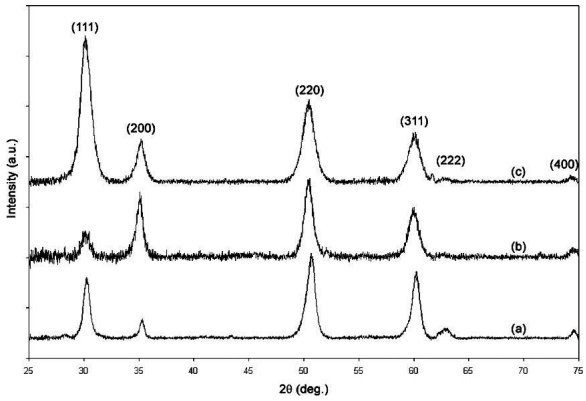

FIG. 1. XRD patterns of thin-film cubic/tetragonal zirconia deposited on Si by PP-MOCVD at different deposition temperatures. (a) 700 °C (b) 655 °C (c) 620 °C. At 620 °C a trace of monoclinic ZrO_2 can be seen at 28°.

Table II summarizes the Zr to O composition of the films determined by EDS. A sample held at 600 °C with no exposure to precursor had only a small amount of oxygen detected on the surface (1.5%). Thicker films of zirconia show the expected 1:2 ratio of Zr to O, but

TABLE II. EDS data of atomic percentages and calculated ratios for zirconia films on Si.

Sample T, pulses	ZrO_2 film thickness (nm)	At.%			Atomic ratios	
		O K	Si K	Zr L	Zr	O
570 °C, 78	100	15.17	81.54	3.29	1	4.6
600 °C, 80	105	11.94	86.16	1.9	1	6.3
500 °C, 300	107	14.65	81.98	3.37	1	4.3
620 °C, 300	525	43.38	35.68	20.94	1	2.1
655 °C, 300	560	40.9	39.06	20.04	1	2.0
700 °C, 300	815	50.06	26.7	23.25	1	2.2
600 °C, 0	⋯	1.46	99.56	−1.03	⋯	⋯

thinner samples (100 nm) may have less accurate measurements, with signal contribution from the silicon substrate. The evaluation of stoichiometry by EDS for thin films is always difficult because of the excitation bulk, and the high oxygen concentration values for thinner films may be caused by this artifact. The EDS also established there was no significant (>2%) carbon remaining in the sample.

B. Grain size and morphology of films

Crystal grain size was calculated by determining the peak broadening in the XRD using the Scherer formula.[27] The calculated grain size decreased from 18 nm at 620 °C, 17 nm at 650 °C, and 11 nm at 700 °C. Analysis of plan-view SEM images in Figs. 2(a) and 2(b) indicated an increase in grain size as temperature increases from 30 nm (500 °C) to 42 nm (700 °C). These results (30–42 nm) are within the same magnitude as XRD crystallite size calculations (11–18 nm), although the XRD data indicate smaller grains at higher temperatures. Typically, XRD estimates a smaller grain size, and in SEM grain sizes are sometimes difficult to resolve. However, both XRD and SEM data clearly show the formation of nanocrystalline zirconia.

TEM cross sections of a zirconia film deposited at 700 °C (300 pulses) in Fig. 3 show bright-field image of zirconia grains with sizes on the order of 10 to 20 nm, agreeing with the XRD data. Figure 4 displays the corresponding selected area diffraction pattern with diffracting planes that index as cubic ZrO_2. The presence of diffraction rings indicates a very small crystallite size. The diffraction rings also show no preferred orientation

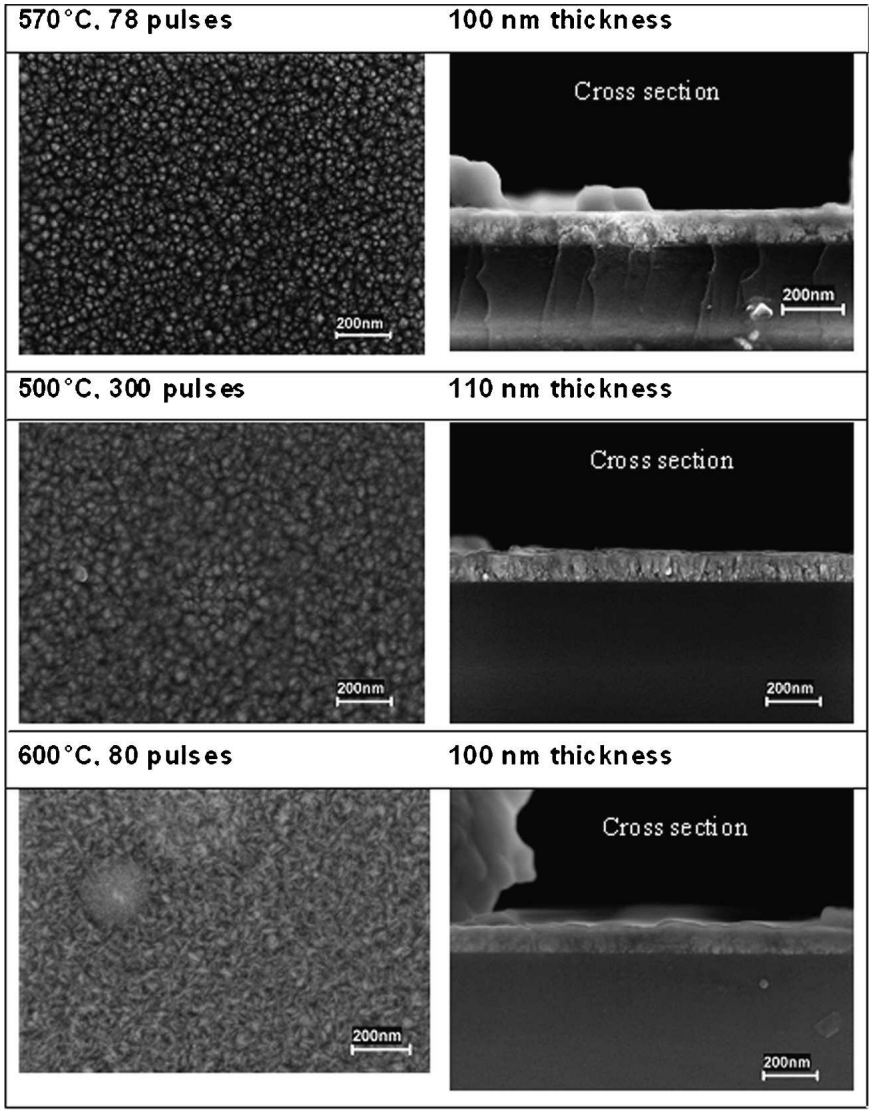

(a)

FIG. 2. SEM micrographs (a) and (b) of surface and cross-sectional views of zirconia films on Si; (b) shows columnar growth structures.
(continued on next page)

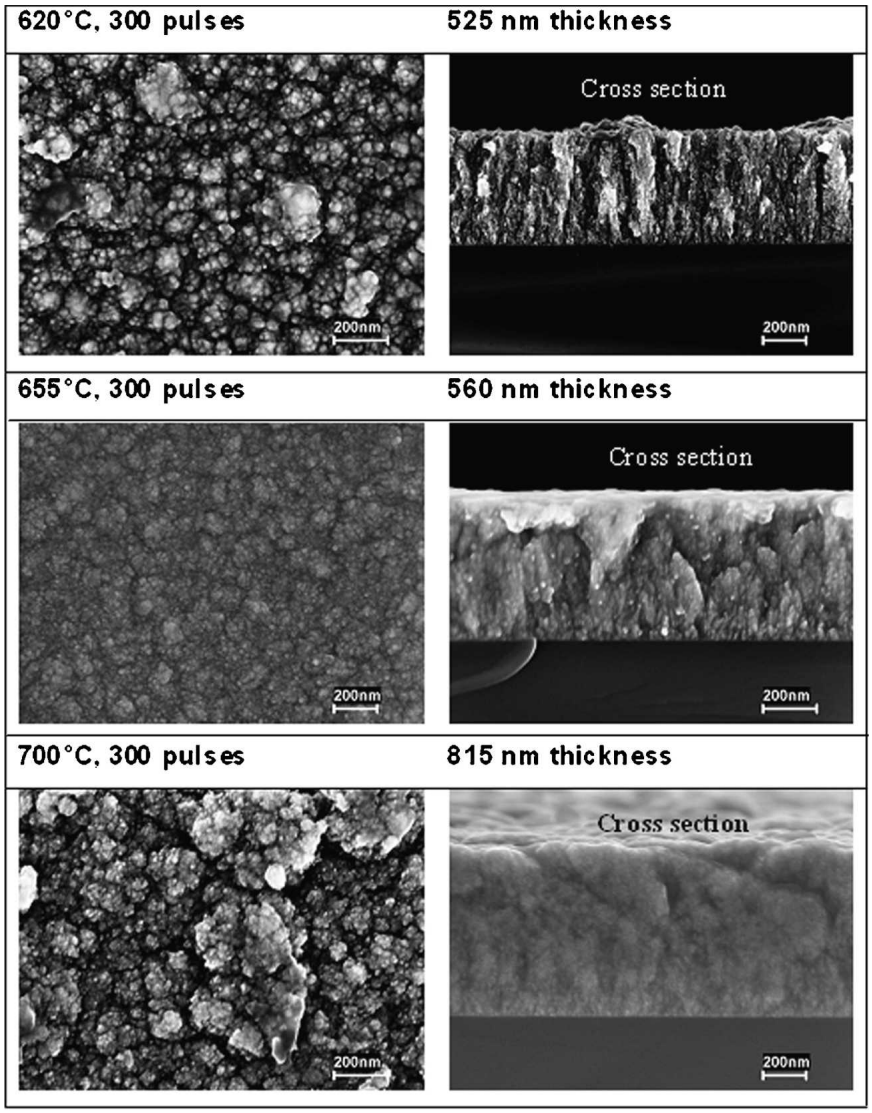

FIG. 2. *(continued)*

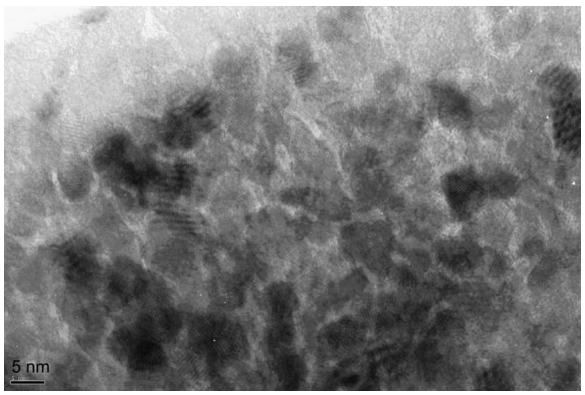

FIG. 3. TEM micrograph of zirconia film of thickest sample (700 °C, 300 pulses).

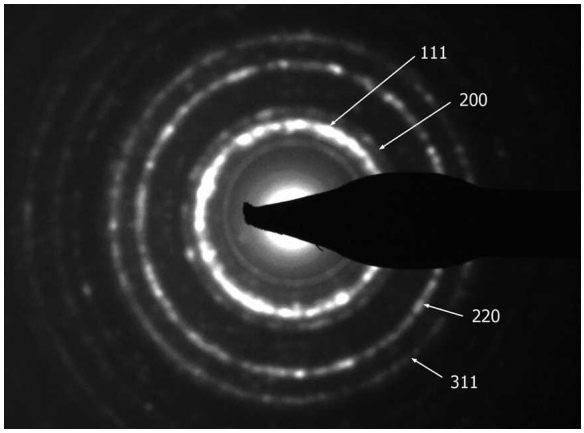

FIG. 4. Selected-area diffraction (SAD) pattern of zirconia film deposited at 700 °C with 300 pulses.

for the 700 °C sample, consistent with the random orientation determined from the XRD data.

SEM cross sections for the sample grown at 620 °C reveal not only nanocrystalline grains, but also a columnar growth structure [Fig. 2(b)]. Zirconia films grown by other CVD techniques at comparable temperatures have a nanocrystalline grain size that is similar,[28,29] although most films exhibit a mixture of monoclinic and tetragonal phases with some indication of preferred orientation. One paper reported the growth of extremely large zirconia grains of 5 to 8 μm using MOCVD,[30] but upon examination of the SEM data presented, the columns of zirconia appear to be on the order of 100 nm in width.

The film morphology did not differ much within the temperature range of this study. Seventy-eight pulse films have the same crystal size as the 300 pulse films, in the range of 10 to 20 nm, and exhibit only a slight variation with deposition temperature. The biggest difference with respect to temperature (aside from film thickness) observed in plan-view SEM images were slightly rougher films with some zirconia agglomerates at the film surface at high substrate temperatures. This could be attributed to a faster decomposition of the precursor molecule before its impact with the substrate surface and the premature formation of zirconia.

C. Growth rate and activation energy

SEM cross sections in Figs. 2(a) and 2(b) were used to measure film thickness for the 300 pulse depositions. The average thickness ranged from 100 to 815 nm. The maximum deposition rate of approximately 3 nm per pulse was achieved at 700 °C. The lowest growth rate was at the lowest temperature, 500 °C, with an average growth rate of 0.4 nm per pulse. Intermediate temperatures yielded average deposition rates between 1 to 2 nm per pulse. Increasing the substrate temperature increases the reaction and decomposition of the precursor and increases film-growth rates. Growth rates ranged from 0.1 μm/h at 500 °C to 1.0 μm/h at 700 °C. Reported values for other MOCVD processes of zirconia are within this same growth rate range at similar temperatures.[16,23,29,31] PP-MOCVD growth occurs during a fraction of the entire pulse time, as opposed to a continuous MOCVD growth, so the reported growth rate for PP-MOCVD will be different than normally reported.

Figure 5 plots the log of film growth versus inverse temperature. The growth rate follows an Arrhenius function with an activation energy obtained by the slope of 42 ± 5 kJ/mol. This is similar to activation energies for similar zirconia precursors reported elsewhere.[31–33] This relatively low activation energy suggests a surface-reaction-limited process as proposed by Chour et al.[34] In contrast, for conventional atmospheric MOCVD, the precursor diffusion rate in the carrier gas is often the rate-limiting step.

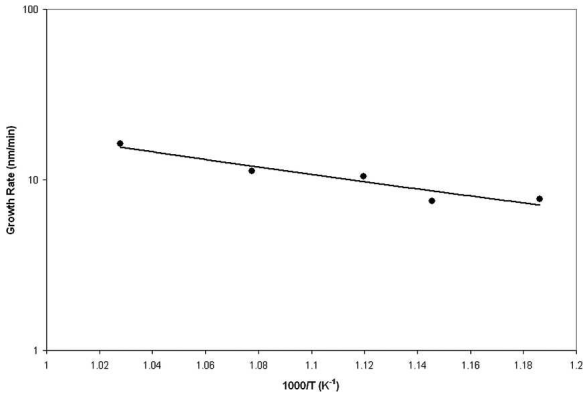

FIG. 5. Plot of growth rate (GR) versus temperature.

The temperature measurement from the thermocouple in the susceptor plate was steady and repeatable. The actual substrate temperature can be substantially lower than the susceptor for a cold-walled reactor, as is the case for all CVD, and the difference depends on the pressure. In PP-MOCVD, the substrate temperature pulses upward with the pressure pulse while the measured temperature at the susceptor stays constant. However, the measured temperature should be used as an indication of the processing conditions and not as an exact deposition temperature.

D. Nucleation and growth

Samples with a small number of pulses (1–15) of zirconia precursor on silicon were used to study initial film development. Figure 6 shows a SEM backscattered image of early film growth. This image displays a large zirconia island (100 nm) on silicon substrate after one 50 μL pulse of precursor at 700 °C. There is also a fine structure in the background of 10 to 20 nm particles. The sample remained heated for several minutes after the pulse, then was cooled slowly under vacuum. This zirconia island is an order of magnitude larger than the

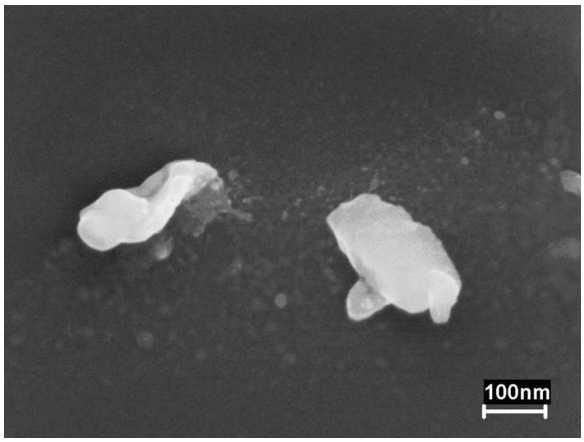

FIG. 6. SEM ESB micrograph of zirconia islands on silicon substrate (700 °C, 1 pulse).

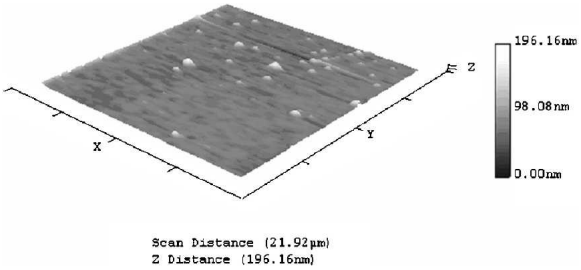

FIG. 7. Three-dimensional output for AFM scan showing ZrO_2 islands from 1 pulse of precursor at 700 °C on Si substrate.

average film grain size determined for the film deposited over 300 pulses. While crystallography of these individual crystals is not practical, EDS analysis indicated that they are zirconia.

The early film growth shown in Fig. 6 is representative of many "first crystals" from several other one-pulse experiments. We hypothesize several possible routes of formation for this inhomogeneous nucleation. First, the large crystal could have formed from a droplet of precursor that fell onto the substrate without evaporating. Measurements obtained from AFM analysis show these "first crystals" formed with an average height of 90 to 100 nm (Fig. 7). The particle analysis obtained by AFM, shown in Table III, has been used to calculate the amount of ZrO_2 material contained in a single island. Assuming the island is cubic zirconia, the volume is multiplied by the density, then divided by the molecular weight to determine the mol content in one island. The droplet volume is calculated from the droplet diameter (20 μm), and mol content is similarly determined, assuming full conversion of precursor to zirconia. Based on these calculations, it has been determined that the island size is 3 orders of magnitude smaller than the zirconia particle that would result if an island were to have formed from an unevaporated rogue droplet of precursor. The conclusion from this observation is that the islands are not forming from the direct impingement of liquid droplets on the substrate surface.

Alternatively, since this is the first liquid through the nozzle, it is possible that a small piece of dried precursor was dislodged from the nozzle and fell onto the substrate or droplets formed zirconia powder in the vapor above the substrate. However, the individual crystals are relatively adherent to the substrate and cannot be removed with dust-removal nitrogen flow. Thus we conclude that the large single crystals were grown on the surface rather than falling there.

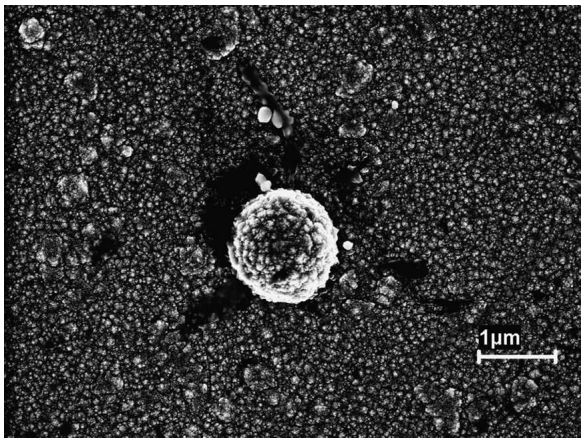

FIG. 8. SEM top view of zirconia film with agglomerations at the surface.

A third possibility is that the precursor adsorbed on the surface is highly mobile during the heating and decomposition processes, even after complete decomposition reaction to ZrO_2, and so the mobile adatoms diffuse across the silicon surface readily until they encounter a nucleation site. In this manner, a single nucleation site could collect the available adsorbed material and become large. We have observed occasional large crystals in the 300 pulse thin films, as illustrated in Fig. 8, which could be remnant initiation crystals.

The nucleation of isolated particles suggest a possible Volmer–Weber growth mode in which precursor molecules preferentially adhere to nucleation sites rather than uniformly nucleate across the substrate surface. Surface flaws in the silicon substrate have been observed to serve as preferential nucleation sites. Figure 9 shows a row of particles grown after 15 pulses at 700 °C, nucleating at a surface scratch. If the arriving molecules preferentially attach to preexisting islands and grow normal to the surface rather than along the surface, atomically smooth thin-film growth is not possible and PP-MOCVD would not satisfy the ultrathin and ultra-uniform film requirements for microelectronic gate oxide thickness (about 5 nm). One could modify the PP-MOCVD process to obtain smoother films by lowering the temperature of the substrate, thus decreasing the tendency of the precursor to stick to itself and allowing the precursor to cover more of the substrate, which would result in a smoother, thinner film.

The shot volume and concentration determines the maximum pressure of the system. By decreasing the shot

TABLE III. Particle analysis from AFM scan using NanoRule+ software from Pacific Nanotech.

Particle analysis	Area (μm^2)	Perimeter (μm)	Volume (μm^3)	Height (nm)	Radius (μm)	Length (μm)	Width (μm)	Aspect ratio
Average	0.24	1.50	0.024	92.62	0.19	0.58	0.31	1.81
Standard deviation	0.16	0.66	0.022	17.91	0.09	0.24	0.14	0.69

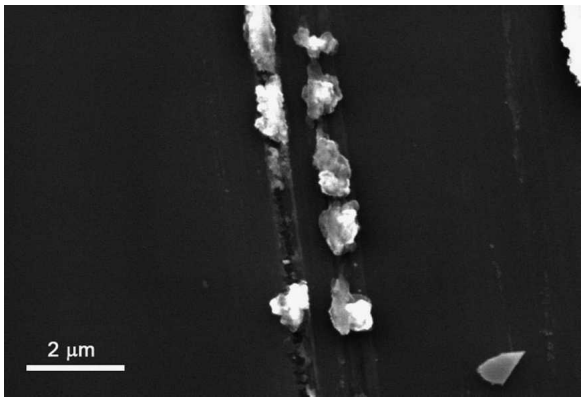

FIG. 9. SEM micrograph of nucleation clusters of ZrO_2 at Si surface flaws from PP-MOCVD of 15 pulses at 700 °C.

volume from 50 to 20 μL per pulse, and keeping the concentration the same, the maximum pressure of the system was reduced from 550 to 330 Pa. The pressure change did not seem to affect the initial stages of film growth, as there was no indication of a difference in island size between the low-pulsed samples with shot volumes of 50 or 20 μL. It was difficult to determine if the density of zirconia islands differed in these samples because the islands were inhomogeneously distributed.

From the observations we have made, we propose a nucleation and growth initiation model for PP-MOCVD that is somewhat different from the classical island growth model. The model is illustrated in Fig. 10. On a clean, single-crystal silicon substrate with few flaws or crystal edges in the surface, adsorbed and decomposing precursor molecules would be highly mobile. On such a substrate, the zirconia molecule would also be relatively mobile. After one pulse exposure more than a monolayer of precursor may have arrived at the substrate and been adsorbed, but because the decomposition reaction is coincident with the arrival, there are not sufficient zirconia molecules across the surface to reach the critical nucleation radius for granular nucleation at many points (islands) or to form a continuous epitaxial layer [Fig. 10(a)]. The adsorbed and decomposing precursor molecules would have high vibration energy due to the high temperature [Fig. 10(b)] and the evolution of reactant product vapor. Clearly, the reaction product hydrocarbons evaporate readily from the surface as no carbon has been identified in any of the PP-MOCVD films.

The decomposing precursor molecules preferentially bond to any crystal ledge in the substrate surface. These molecules bonded to defects in the surface result in a local zirconia concentration sufficient for nucleation [Fig. 10(c)]. The nucleated zirconia crystal continues to accumulate both decomposing precursor molecules and adsorbed mobile zirconia molecules that are diffusing across the silicon surface. During the relaxation time between the first few pulses, most of the adsorbed precursor and zirconia is effectively assimilated into the single crystal growth sites, leaving a low concentration of zirconia on the surface (too low for detection) [Fig. 10(d)]. The process is repeated for the second pulse, but the concentration of amorphous (noncrystallized) zirconia molecules on the surface increases with each pulse, and new nucleation sites arise from the presence of the

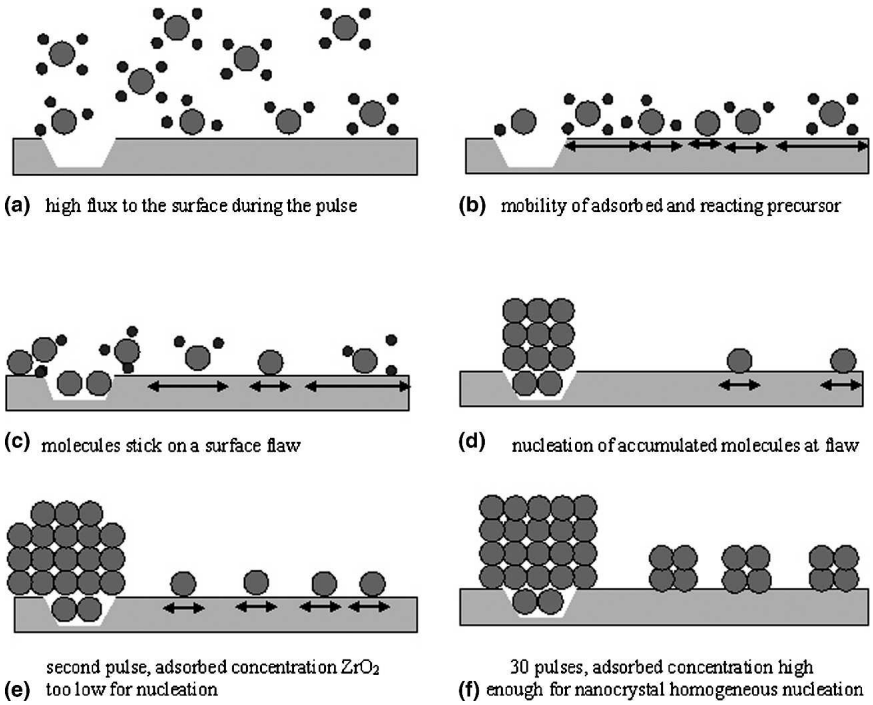

FIG. 10. PP-MOCVD nucleation and growth initiation model. See text for details.

adsorbed zirconia [Fig. 10(e)]. After several pulses, sufficient zirconia is present on the surface to allow local nucleation as individual nanocrystals [Fig. 10(f)].

In a conventional LP-MOCVD process without a relaxation time, the arrival rate would be lower but continuous. There may not be sufficient material to form the large single crystals we have observed. As other studies of the first stages of vapor exposure and growth are not reported, we cannot really postulate whether the formation of large crystals does or does not occur in other steady-flow MOCVD processes. However, the presence of occasional, large grains has been frequently observed in films deposited with a variety of methods.[35,36]

IV. CONCLUSIONS

PP-MOCVD was used to study the first stages of nucleation and growth of zirconia on single crystal silicon substrates. This method can produce nanocrystalline films of cubic/tetragonal zirconia. Substrate temperature is the primary factor affecting film growth rate and, to some degree, film morphology. Complete substrate coverage was achieved with no visible porosity for thin films of 40 to 800 nm thick, grown at temperatures of 500 to 700 °C, with growth rates of 0.1 to 1 μm/h. These preliminary results indicate that the experimental conditions nucleate by a Volmer–Weber mechanism and produce films that may potentially be used in fuel cells or thermal-barrier coatings. The growth of ultrathin epitaxial or polycrystalline films with minimal roughness would require high-quality, flaw-free substrates and the use of low deposition temperatures.

ACKNOWLEDGMENTS

The authors wish to acknowledge the Carl Zeiss Center of Excellence in Electron Microscopy at the University of California, Irvine. A portion of this work was supported by IRL, and graduate support was provided by a GAANN fellowship, the NSF/AGEP, and the Hispanic Scholarship fund. The authors would also like to recognize Asdis Krisindottir, Vi Siriwongrungson, Mike Flaws, and Nick Long for their contribution to this project.

REFERENCES

1. J.P. Chang, Y.S. Lin, and K. Chu: Rapid thermal chemical vapor deposition of zirconium oxide for metal-oxide-semiconductor field effect transistor application. *J. Vac. Sci. Technol., B* **19,** 1782 (2001).
2. M. Fakhruddin, R. Singh, K.F. Poole, S.V. Kondapi, and J. Narayan: The effect of interfacial layers on high-performance gate dielectrics processed by RTP-ALD. *J. Electrochem. Soc.* **151,** G507 (2004).
3. S. Ramanathan and P.C. McIntyre: Ultrathin zirconia/SiO_2 dielectric stacks grown by ultraviolet-ozone oxidation. *Appl. Phys. Lett.* **80,** 3793 (2002).
4. J. Wang, L. Zhao, N.H. Luu, D. Wang, and H. Nakashima: Structural and electrical properties of Zr oxide film for high-k gate dielectrics by using electron cyclotron resonance plasma sputtering. *Appl. Phys. A, Mater.* **80,** 1781 (2005).
5. S.H. Jeong, I.S. Bae, Y.S. Shin, S.B. Lee, H.T. Kwak, and J.H. Boo: Physical and electrical properties of ZrO_2 and YSZ high-k gate dielectric thin films grown by RF magnetron sputtering. *Thin Solid Films* **475,** 354 (2005).
6. L.B. Chen: Yttria-stabilized zirconia thermal-barrier coatings—A review. *Surf. Rev. Lett.* **13,** 535 (2006).
7. U. Schulz, B. Saruhan, K. Fritscher, and C. Leyens: Review on advanced EB-PVD ceramic topcoats for TBC applications. *Int. J. Appl. Ceram. Technol.* **1,** 302 (2004).
8. T.A. Dobbins, R. Knight, and M.J. Mayo: HVOF thermal spray deposited Y_2O_3-stabilized ZrO_2 coatings for thermal barrier applications. *J. Therm. Spray Technol.* **12,** 214 (2003).
9. B. Goswami, S.K. Sahay, and A.K. Ray: Application of thermal-barrier coatings on combustion chamber liners—A review. *High Temp. Mater. Pr.-Isr.* **23,** 211 (2004).
10. F. Tang and J.M. Schoenung: Evolution of Young's modulus of air plasma sprayed yttria-stabilized zirconia in thermally cycled thermal-barrier coatings. *Scr. Mater.* **54,** 1587 (2006).
11. G. Wahl, C. Metz, and S. Samoilenkov: Thermal-barrier coatings. *J. Phys. [E] IV* **11,** 835 (2001).
12. P. Von Dollen and S. Barnett: A study of screen printed yttria-stabilized zirconia layers for solid oxide fuel cells. *J. Am. Ceram. Soc.* **88,** 3361 (2005).
13. S. Krumdieck, O. Sbaizero, and R. Raj: Unique precursor delivery and control afforded by low-pressure pulsed-CVD process with ultrasonic atomization. *J. Phys. [E] IV* **11,** 1161 (2001).
14. S. Krumdieck and R. Raj: Conversion efficiency or alkoxide precursor to oxide films grown by an ultrasonic-assisted, pulsed liquid injection, metalorganic chemical vapor deposition (pulsed-CVD) process. *J. Am. Ceram. Soc.* **82,** 1605 (1999).
15. H.M. Cave, S.P. Krumdieck, and M.C. Jermy: Development of a model for high precursor conversion efficiency pulsed-pressure chemical vapor deposition (PP-CVD) processing. *Chem. Eng. J.* **135,** 120 (2008).
16. M.A. Cameron and S.M. George: ZrO_2 film growth by chemical vapor deposition using zirconium tetra-tert-butoxide. *Thin Solid Films* **348,** 90 (1999).
17. Y. Kajikawa and S. Noda: Growth mode during initial stage of chemical vapor deposition. *Appl. Surf. Sci.* **245,** 281 (2005).
18. S. Krumdieck and R. Raj: Growth rate and morphology for ceramic films by pulsed-MOCVD. *Surf. Coat. Technol.* **141,** 7 (2001).
19. S.P. Krumdieck, O. Sbaizero, A. Bullert, and R. Raj: Solid yttria-stabilized zirconia films by pulsed chemical vapor deposition from metal–organic precursors. *J. Am. Ceram. Soc.* **85,** 2873 (2002).
20. P.A. Williams, J.L. Roberts, A.C. Jones, P.R. Chalker, N.L. Tobin, J.F. Bickley, H.O. Davies, L.M. Smith, and T.J. Leedham: Novel mononuclear alkoxide precursors for the MOCVD of ZrO_2 and HfO_2 thin films. *Chem. Vap. Deposition* **8,** 163 (2002).
21. W.S. Rasband: ImageJ, in U.S. National Institutes of Health, (Bethesda, MD, 1997–2006).
22. L. Weaver: Cross-section TEM sample preparation of multilayer and poorly adhering films. *Microsc. Res. Technol.* **36,** 368 (1997).
23. D.J. Burleson, J.T. Roberts, W.L. Gladfelter, S.A. Campbell, and R.C. Smith: A study of CVD growth kinetics and film microstructure of zirconium dioxide from zirconium tetra-tert-butoxide. *Chem. Mater.* **14,** 1269 (2002).

24. S. Mathur, J. Altmayer, and H. Shen: Nanostructured ZrO_2 and Zr–C–N coatings from chemical vapor deposition of metal-organic precursors. *Z. Anorg. Allg. Chem.* **630,** 2042 (2004).
25. Powder Diffraction File, Card No. 30-1468 and Card No. 17-0923, (Joint Committee on Powder Diffraction Standards, Swathmore, PA).
26. R. Tu, T. Kimura, and T. Goto: High-speed deposition of yttria stabilized zirconia by MOCVD. *Surf. Coat. Technol.* **187,** 238 (2004).
27. B.E. Warren: *X-Ray Diffraction* (Addison-Wesley, London, 1969).
28. G.Y. Meng, H.Z. Song, Q. Dong, and D.K. Peng: Application of novel aerosol-assisted chemical vapor deposition techniques for SOFC thin films. *Solid State Ionics* **175,** 29 (2004).
29. O. Bernard, A.M. Huntz, M. Andrieux, W. Seiler, V. Ji, and S. Poissonnet: Synthesis, structure, microstructure and mechanical characteristics of MO CVD deposited zirconia films. *Appl. Surf. Sci.* **253,** 4626 (2007).
30. J.A. Belot, R.J. McNeely, A. Wang, C.J. Reedy, T.J. Marks, G.P.A. Yap, and A.L. Rheingold: Expedient route to volatile zirconium metal-organic chemical vapor deposition precursors using amide synthons and implementation in yttria-stabilized zirconia film growth. *J. Mater. Res.* **14,** 12 (1999).
31. G. Garcia, J. Caro, J. Santiso, J.A. Pardo, A. Figueras, and A. Albrutis: Pulsed injection MOCVD of YSZ thin films onto dense and porous substrates. *Chem. Vap. Deposition* **9,** 279 (2003).
32. S.A. Shivashankar and M.S. Dharmaprakash: Effect of nature of the precursor on crystallinity and microstructure of MOCVD-grown ZrO_2 thin films, in *Novel Materials and Processes for Advanced CMOS,* edited by M.I. Gardner, S. De Gendt, J-P. Maria, and S. Stemmer (Mater. Res. Soc. Symp Proc. **745,** Warrendale, PA, 2003), pp. 191–196.
33. S.P. Krumdieck, O. Sbaizero, A. Bullert, and R. Raj: YSZ layers by pulsed-MOCVD on solid oxide fuel cell electrodes. *Surf. Coat. Technol.* **167,** 226 (2003).
34. K.W. Chour, J. Chen, and R. Xu: Metal-organic vapor deposition of YSZ electrolyte layers for solid oxide fuel-cell applications. *Thin Solid Films* **304,** 106 (1997).
35. I.H. Jung, K.K. Bae, M.S. Yang, and S.K. Ihm: A study of the microstructure of yttria-stabilized zirconia deposited by inductively coupled plasma spraying. *J. Therm. Spray Technol.* **9,** 463 (2000).
36. P. Dahl, I. Kaus, Z. Zhao, M. Johnsson, M. Nygren, K. Wiik, T. Grande, and M.A. Einarsrud: Densification and properties of zirconia prepared by three different sintering techniques. *Ceram. Int.* **33,** 1603 (2007).